

Phase separation and Si nanocrystal formation in bulk SiO studied by x-ray scattering

O. M. Feroughi, C. Sternemann, Ch. J. Sahle, M. A. Schroer, H. Sternemann et al.

Citation: *Appl. Phys. Lett.* **96**, 081912 (2010); doi: 10.1063/1.3323106

View online: <http://dx.doi.org/10.1063/1.3323106>

View Table of Contents: <http://apl.aip.org/resource/1/APPLAB/v96/i8>

Published by the *AIP Publishing LLC*.

Additional information on *Appl. Phys. Lett.*

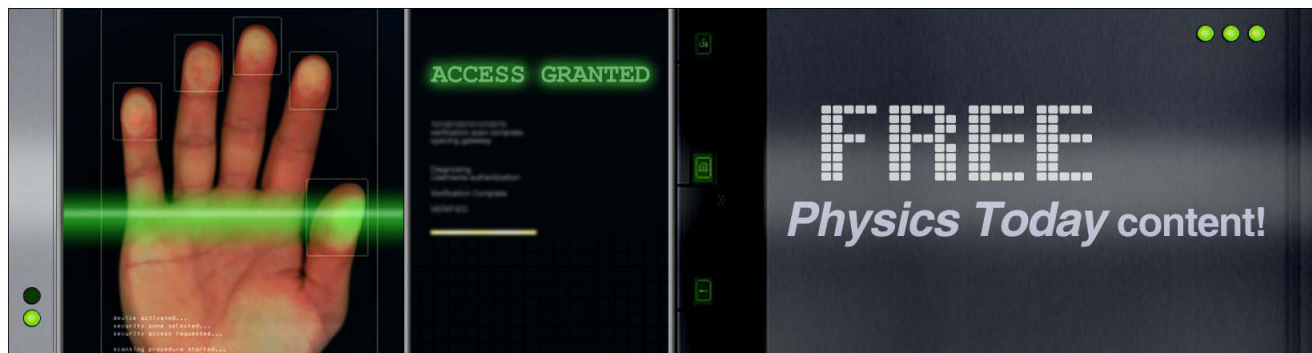
Journal Homepage: <http://apl.aip.org/>

Journal Information: http://apl.aip.org/about/about_the_journal

Top downloads: http://apl.aip.org/features/most_downloaded

Information for Authors: <http://apl.aip.org/authors>

ADVERTISEMENT



Phase separation and Si nanocrystal formation in bulk SiO studied by x-ray scattering

O. M. Feroughi,¹ C. Sternemann,^{1,a)} Ch. J. Sahle,¹ M. A. Schroer,¹ H. Sternemann,¹ H. Conrad,¹ A. Hohl,² G. T. Seidler,³ J. Bradley,³ T. T. Fister,^{3,4} M. Balasubramanian,⁴ A. Sakko,⁵ K. Pirkkalainen,⁵ K. Hämäläinen,⁵ and M. Tolan¹

¹Fakultät Physik/DELTA, Technische Universität Dortmund, 44221 Dortmund, Germany

²Institute for Materials Science, Darmstadt University of Technology, 64287 Darmstadt, Germany

³Department of Physics, University of Washington, Seattle, Washington 98195, USA

⁴X-ray Science Division, Argonne National Laboratory, Argonne, Illinois 60439, USA

⁵Department of Physics, University of Helsinki, Helsinki, P.O. Box 64, FI-00014, Finland

(Received 19 December 2009; accepted 27 January 2010; published online 23 February 2010)

We present an x-ray scattering study of the temperature-induced phase separation and Si nanocrystal formation in bulk amorphous SiO_x with $x \approx 1$. X-ray Raman scattering at the Si L_{II,III}-edge reveals a significant contribution of suboxides present in native amorphous SiO. The suboxide contribution decreases with increasing annealing temperature between 800–1200 °C pointing toward a phase separation of SiO into Si and SiO₂ domains. In combination with x-ray diffraction and small angle x-ray scattering the SiO microstructure is found to be dominated by internal suboxide interfaces in the native state. For higher annealing temperatures above 900 °C growth of Si nanocrystals with rough surfaces embedded in a silicon oxide matrix can be observed. © 2010 American Institute of Physics. [doi:10.1063/1.3323106]

Bulk amorphous silicon monoxide (a-SiO_x with $x \approx 1$) is a promising material regarding the search for materials in (opto)electronics and semiconductor technology. Structures containing Si nanocrystallites in an oxide matrix are valuable alternatives to fragile, porous Si on the way toward highly efficient photoluminescence devices utilizing Si-based materials.^{1,2} Amorphous SiO shows a phase separation (disproportionation) under annealing combined with a growth of Si and SiO₂ domains. Therefore, it has attracted great interest as a starting material for the production of photoluminescent structures.^{3,4} By phase separation within superlattices of SiO/SiO₂, even a size-controlled growth of Si nanocrystals (NCs) could be achieved.⁵ The structural characterization of amorphous silicon/oxygen systems and their behavior during annealing is therefore of special relevance. Although the optical properties of such systems have been intensively investigated, detailed spectroscopic studies of the underlying electronic and atomic structure are still rare.^{6–9}

In this article, we present a study of the temperature-induced phase separation and Si NC formation in bulk SiO by nonresonant x-ray Raman scattering (XRS), x-ray diffraction (XRD), and small angle x-ray scattering (SAXS). XRS¹⁰ measurements of the Si L_{II,III}-edge are highly sensitive to the chemical environment, e.g., the different oxidation states, of the Si atoms in SiO.¹¹ We probe the variation in the suboxide contribution [i.e., Si(Si_{4–n}O_n) with $n=1, 2, 3$] in SiO during annealing which permits estimates for temperature ranges where the phase separation proceeds and where it is almost completed. We estimate the crystallization temperature and NC sizes by XRD and use SAXS to analyze fractal correlations, which yield information about the microscopic structure of the system.¹²

The amorphous SiO samples were prepared in a vacuum chamber by evaporation of a 1:1 Si/SiO₂ powder mixture

heated to approximately 1400 °C and subsequent deposition of bulk condensates on a cooled surface mounted in the chamber at a condensation temperature of about 600 °C. With a high deposition rate of 200 nm/s bulk thicknesses of several mm were achieved. The native a-SiO samples in bulk pieces were annealed for one hour using a tube furnace and nitrogen flow. Three different sample series were prepared. a-SiO of series A was annealed at 725, 800, 850, 900, 1050, 1100, and 1200 °C, series B at 800, 850, 1050, and 1150 °C, and series C at 800 and 1000 °C. Afterwards the samples were ground to produce powders. The XRS spectra were measured at the Advanced Photon Source (APS) beamline XOR/PNC 20-ID employing the LERIX spectrometer¹³ for momentum transfers q of 2.4 Å⁻¹ (series A), 9.85 Å⁻¹ (series A), and 10.1 Å⁻¹ (series B and C) with energy resolutions of 0.6 eV (series A) and 1.4 eV (series B and C) at a fixed analyzer energy of 9.89 keV by variation in the incident energy. The Si L_{II,III}-edges were extracted from the raw XRS data sets (see Ref. 14) and have been normalized by the area between energy losses of 95 and 120 eV. XRD and SAXS measurements were carried out at beamline BL9 of DELTA¹⁵ using a MAR image plate detector with an incident energy of 27 and 10 keV, respectively.

The structure of native a-SiO can be described as a disproportionation in the initial state, where nanometer-scale Si and SiO₂ domains are separated by suboxide interfaces.⁶ Thus, a significant amount of suboxides in the native sample related to such internal interfaces is expected. The contribution of these interfaces decreases with increasing annealing temperature by further disproportionation. Here, XRS is a unique probe of such internal interfaces¹¹ and allows us to study the phase separation in detail. XRS spectra measured at the Si L_{II,III}-edge of differently annealed SiO samples are shown in Fig. 1(a) for series A measured at high q . Distinct differences between native and annealed samples can be observed in the energy-loss range between 101 and 110 eV. In

^{a)}Electronic mail: christian.sternemann@tu-dortmund.de.

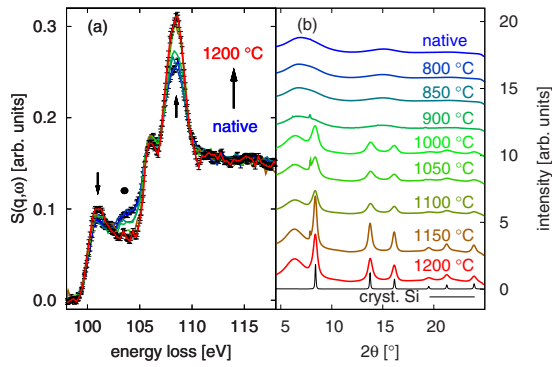


FIG. 1. (Color online) (a) XRS spectra at the Si $L_{II,III}$ -edge of SiO measured for the native state and for different annealing temperatures at high momentum transfer (sample series A, $q=9.85 \text{ \AA}^{-1}$). Spectral features related to suboxide contributions (dot), Si (left arrow), and SiO_2 (right arrow) are indicated. (b) XRD patterns of native and annealed SiO samples. As a reference the XRD pattern of polycrystalline Si is shown.

particular, the strong spectral feature related to suboxide contributions in the bulk material¹¹ between 102 and 106 eV vanishes with increasing annealing temperature. This is accompanied by the increase of both, the peak at 101 eV characteristic for crystalline Si and the white line typical for pure SiO_2 at 108.5 eV. Spectral changes at the Si $L_{II,III}$ -edge onset related to partial crystallization of the amorphous Si phase have been reported earlier¹⁶ but are negligible compared to the observed changes of the suboxide contribution in our XRS spectra. It should be noted that a deeper analysis of the XRS line shapes in comparison with theory allows to study in more detail the underlying electronic structure of suboxide contributions.¹⁷ Although the matrix elements contributing to the XRS spectrum at high q are rather different from photon absorption, the key point is that the XRS process is bulk sensitive and linear, i.e., admixture of different phases results in proportional admixture of spectra. Thus the phase separation can be quantified by calculating the so-called phase separation parameter $A(T)$, which is estimated by the integral of the absolute value of the difference between the spectra of native and annealed samples for the energy loss range 99–106.5 eV where the suboxide contributions dominate the spectral changes. This parameter describes disproportionation as discussed earlier for bulk a-GeO using x-ray absorption.^{18,19} $A(T)=1$ refers to a 1:1 superposition of XRS spectra of Si and SiO_2 as a model for a disproportionated SiO sample and the error bars are estimated based on the statistical accuracy of the XRS measurements. Results are presented in Fig. 2 for the different sample series measured at large (series A, B, C) and small q (series A). The phase separation proceeds at 900 °C and is almost completed at 1200 °C. The XRS measurements clearly indicate that the suboxide content significantly decreases for annealed samples. It was observed in a former study of bulk a-GeO that the temperature-induced phase separation is followed by formation of Ge and, at higher temperatures, GeO_2 NCs.¹⁹ Thus we characterized the native and annealed SiO samples by XRD. The corresponding diffraction patterns are shown in Fig. 1(b) together with a reference spectrum of polycrystalline Si. Due to surface oxidation during annealing a few samples, mainly of series B, show small impurities of crystalline SiO_2 . These effects are non-systematic with temperature and the corresponding SiO_2 Bragg peaks have only a

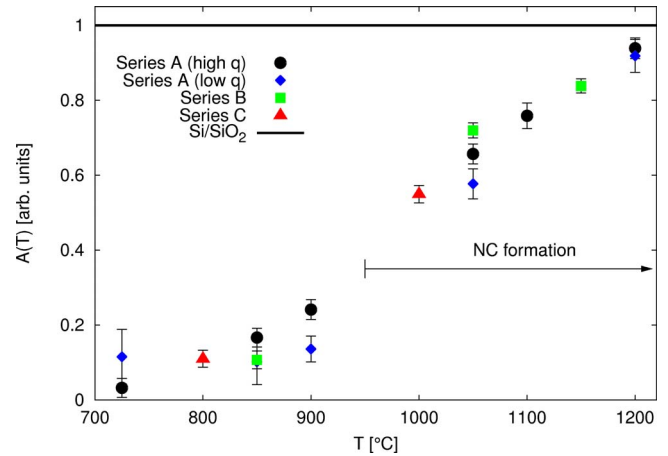


FIG. 2. (Color online) Phase separation parameter $A(T)$ of SiO extracted from XRS spectra measured for sample series A, B, C at high and for A at low momentum transfer. Si/SiO₂ indicates the reference for a fully disproportionated sample. The regime of Si NC formation is shown by the arrow.

negligible integral contribution to the overall XRD pattern. The native samples are found to be amorphous, i.e., they exhibit no long-range order of the atomic arrangement. For annealing temperatures above 900 °C partial Si NC formation is observed. Using the Scherrer equation the average size of the NCs is estimated to $4.0 \pm 0.4 \text{ nm}$ for 1000 °C and increases up to $6.8 \pm 0.7 \text{ nm}$ at 1200 °C in good agreement with former results.²⁰ Thus it can be concluded that the averaged size of Si clusters in the native samples is significantly smaller than 4 nm which supports a strong contribution of suboxides in native SiO. SiO_2 NCs do not form in bulk SiO up to 1200 °C in contrast to GeO, in which GeO_2 crystallites form already 100 °C above the onset of Ge crystallization.¹⁹ This results in a broader temperature window where the size of Si NCs embedded in an amorphous silicon oxide matrix can be tuned without crystallization of SiO_2 . Moreover, the crystallization of Si in SiO sets in before phase separation is completed. The results of the SAXS measurements are presented in Fig. 3(a) for series A. The spectra exhibit a significant temperature dependence whereas the strongest change can be observed across the crystallization temperature of 900 °C. For the two highest annealing temperatures the SAXS pattern can be interpreted with volume particle size-distributions obtained by a Monte Carlo

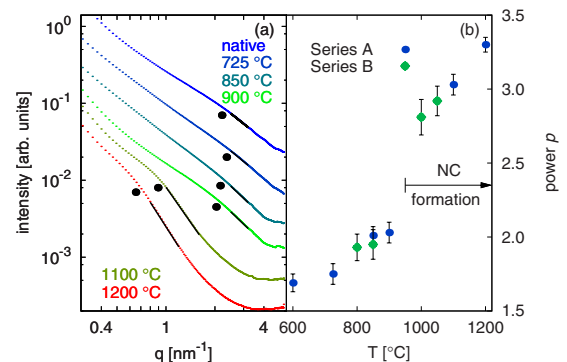


FIG. 3. (Color online) (a) SAXS pattern of native and differently annealed SiO shown for sample series A on a double-logarithmic plot. The fitting ranges to extract the power-law exponent p are indicated as solid lines and the Guinier-to-Porod transition is marked by dots. (b) Resulting p for SAXS measurements of sample series A and B. The regime of Si NC growth is indicated.

method²¹ yielding mean sizes of 7.2 ± 1.0 and 10.4 ± 1.0 nm in line with the XRD results. To access information on the samples' morphology, the SAXS data were further analyzed in terms of fractal correlations estimating the power-law exponent p by the slope of $\ln I$ against $\ln q$ in the Porod regime,¹² where I is the SAXS intensity and $q=4\pi/\lambda \sin(2\Theta/2)$ with wavelength λ and the scattering angle 2Θ . Values of $3 \leq p \leq 4$ refer to scattering at surface fractals, e.g., compact particles with a rough surface, and values of $p \leq 3$ to scattering at mass fractals, e.g., colloidal aggregates or two phase systems with ramified domains. The fitting ranges used to calculate p are indicated in Fig. 3(a) by solid lines and are restricted to the regimes of linear decrease in $\ln I$. The transition from the Guinier to the Porod regime is indicated by dots. The power-law exponent p of differently annealed SiO samples for series A and B is shown in Fig. 3(b). Upon annealing the fractal dimensions describing the microstructure of the SiO samples changes from mass fractals to surface fractals in the NC regime. In particular the value of p shows a significant rise at the onset temperature for formation of Si NCs and an increase with crystal size, indicating the process of crystal growth. In the native samples and for small annealing temperatures values of $p \approx 2$ are estimated pointing toward scattering at mass fractals. This observation can be related to a microstructure of native SiO where internal suboxide interfaces dominate the system. It can be understood as an early stage of disproportionation in the initial state.

In conclusion, we characterized the process of temperature-induced phase separation and Si NC formation in bulk SiO by x-ray scattering methods. During phase separation SiO transforms from a structure which is dominated by suboxide interfaces to a structure in which Si NCs with rough surfaces are embedded in a silicon oxide matrix. The strongest structural changes occur between 900 and 1050 °C. In contrast to bulk GeO, the size of Si NCs can be tuned in the nanometer range over a broad temperature range without crystallization of SiO₂. These findings provide a detailed view on the microscopic structural changes which occur during annealing of SiO on the way to NC formation and thus have impact on the production of NCs embedded in oxide matrices with tunable physical properties.

The authors would like to acknowledge APS and DELTA for providing synchrotron radiation. This work was sup-

ported by DAAD (Grant Nos. 313-PPP-SF/08-IK and 1127504), DFG (Grant No. TO 169/14-1) and the Academy of Finland (Grant Nos. 1110571 and 1127462).

- ¹S. S. Iyer and Y.-H. Xie, *Science* **260**, 40 (1993).
- ²L. Pavesi, L. Dal Negro, C. Mazzoleni, G. Franzo, and F. Priolo, *Nature (London)* **408**, 440 (2000).
- ³V. Kapaklis, C. Politis, P. Pouloupoulos, and P. Schweiss, *Appl. Phys. Lett.* **87**, 123114 (2005).
- ⁴M. Mamiya, H. Takei, M. Kikuchi, and C. Uyeda, *J. Cryst. Growth* **229**, 457 (2001).
- ⁵M. Zacharias, J. Heitmann, R. Scholz, U. Kahler, M. Schmidt, and J. Bläsing, *Appl. Phys. Lett.* **80**, 661 (2002).
- ⁶A. Hohl, T. Wieder, P. A. van Aken, T. E. Weirich, G. Denninger, M. Vidal, S. Oswald, C. Deneke, J. Mayer, and H. Fuess, *J. Non-Cryst. Solids* **320**, 255 (2003).
- ⁷J. J. van Hapert, A. M. Vredenberg, E. E. van Faassen, N. Tomozeiu, W. M. Arnoldbik, and F. H. P. M. Habraken, *Phys. Rev. B* **69**, 245202 (2004).
- ⁸W. M. Arnoldbik, N. Tomozeiu, E. D. van Hattum, R. W. Lof, A. M. Vredenberg, and F. H. P. M. Habraken, *Phys. Rev. B* **71**, 125329 (2005).
- ⁹A. Zimina, S. Eisebitt, W. Eberhardt, J. Heitmann, and M. Zacharias, *Appl. Phys. Lett.* **88**, 163103 (2006).
- ¹⁰See for an overview on XRS: W. Schülke, *Electron Dynamics by Inelastic X-ray Scattering* (Oxford University Press, New York, 2007); C. Sternemann, H. Sternemann, S. Huotari, F. Lehmkuhler, M. Tolan, and J. S. Tse, *J. Anal. At. Spectrom.* **23**, 807 (2008).
- ¹¹C. Sternemann, J. A. Soininen, M. Volmer, A. Hohl, G. Vankó, S. Streit, and M. Tolan, *J. Phys. Chem. Solids* **66**, 2277 (2005).
- ¹²D. W. Schaefer, B. C. Bunker, and J. P. Wilcoxon, *Proc. R. Soc. London, Ser. A* **423**, 35 (1989).
- ¹³T. T. Fister, G. T. Seidler, L. Wharton, A. R. Battle, T. B. Ellis, J. O. Cross, A. T. Macrander, W. T. Elam, T. A. Tyson, and Q. Quian, *Rev. Sci. Instrum.* **77**, 063901 (2006).
- ¹⁴H. Sternemann, C. Sternemann, G. T. Seidler, T. T. Fister, A. Sakko, and M. Tolan, *J. Synchrotron Radiat.* **15**, 162 (2008).
- ¹⁵C. Krywka, C. Sternemann, M. Paulus, N. Javid, R. Winter, A. Al-Sawalimih, S. Yi, D. Raabe, and M. Tolan, *J. Synchrotron Radiat.* **14**, 244 (2007).
- ¹⁶C. Tarrío and S. E. Schnatterly, *J. Opt. Soc. Am. B* **10**, 952 (1993).
- ¹⁷A. Sakko, C. Sternemann, Ch. J. Sahle, H. Sternemann, O. M. Feroughi, H. Conrad, F. Djurabekova, A. Hohl, G. T. Seidler, M. Tolan, and K. Hämäläinen (unpublished).
- ¹⁸A. Schacht, C. Sternemann, A. Hohl, H. Sternemann, C. Sahle, M. Paulus, and M. Tolan, *J. Non-Cryst. Solids* **355**, 1285 (2009).
- ¹⁹C. J. Sahle, C. Sternemann, H. Conrad, A. Herdt, O. M. Feroughi, M. Tolan, A. Hohl, R. Wagner, D. Lützenkirchen-Hecht, R. Frahm, A. Sakko, and K. Hämäläinen, *Appl. Phys. Lett.* **95**, 021910 (2009).
- ²⁰V. M. Burlakov, G. A. D. Briggs, A. P. Sutton, A. Bongiorno, and A. Pasquarello, *Phys. Rev. Lett.* **93**, 135501 (2004).
- ²¹U. Vainio, K. Pirkkalainen, K. Kisko, G. Goerigk, N. E. Kotelnikova, and R. Serimaa, *Eur. Phys. J. D* **42**, 93 (2007).